# The Uniqueness of the Propyl Compound in the Series $(C_nH_{2n+1}NH_3)_2MnCl_4$ with $n = 1$–10

W. DEPMEIER*

*Universität Konstanz, FB Chemie, Postfach 7733, D 7750 Konstanz, Federal Republic of Germany*

The perovskite-like layer structures of $(C_nH_{2n+1}NH_3)_2MnCl_4$ with $n = 1$–10 have been investigated by X-ray methods to determine their lattice constants and the temperature of transition to the respective zero-tilt phases. It has been found that the propyl compound is distinctive in that it exhibits the highest temperature of transition to a zero-tilt phase, the longest Mn–Cl bond, and the largest difference between the $a$ and $b$ lattice parameters. Furthermore, it undergoes a large number of phase transitions (five), some of which are accompanied by the formation of commensurable or incommensurable superstructures. The special position of this compound is attributed to geometrical peculiarities related to the terminal methyl groups. The propyl compound is the only member of the series in which coupled movements of terminal methyl groups of neighboring strata do not seem to be important below 400°K.

## Introduction

The group of compounds $(C_nH_{2n+1} \times NH_3)_2MCl_4$ with $M = $ Mn, Fe, Cd, Cu have been of appreciable interest in recent years owing to their phase-transitional, two-dimensional magnetic, and lattice dynamical properties [for a selection of references, see (1–4)]. Furthermore, these compounds have been considered as possible model structures for biological membranes. The $K_2NiF_4$-type structures consist of layers of corner-sharing $MCl_6$ octahedra. Two corners of each octahedron (not necessarily a regular one) remain free, with each formally carrying a charge of $(-1)$. Thus, the composition of the perovskite-like layer is $MCl_4^{2-}$. The negative charge of the macro-anion is balanced by alkylammonium ions situated on each side of

the layer. In all cases investigated so far, the $NH_3$ residue of these quasi-linear ions has been found to point at the layer and to be situated in a cavity of the layer formed by eight chlorine atoms. Each of these chlorine atoms can act as an acceptor for N–H···Cl hydrogen bonds with which the alkylammonium groups are generally attached to the layers. Thus, neutral strata are formed which stack upon each other. Figure 1 shows a part of the structure of $(C_3H_7NH_3)_2MnCl_4$ (17). Remarkably, the alkyl chains of neighboring strata do not penetrate each other, but have contacts similar to those of phospholipids in a biomembrane (5). Changes in the tilt system (6, 1) of the perovskite layer and in the ordering of the hydrogen bonding schemes together with interactions of the motions of the alkyl chains lead to various structural phase transitions. These phase transitions have been thoroughly investigated for the methyl compounds of Mn and Cd (7–11). For the ethyl compound with Mn (12) and

* Present address: Université de Genève, Département de Chimie Minérale et de Chimie Analytique, 30 quai Ernest Ansermet, CH 1211 Genève, Switzerland.
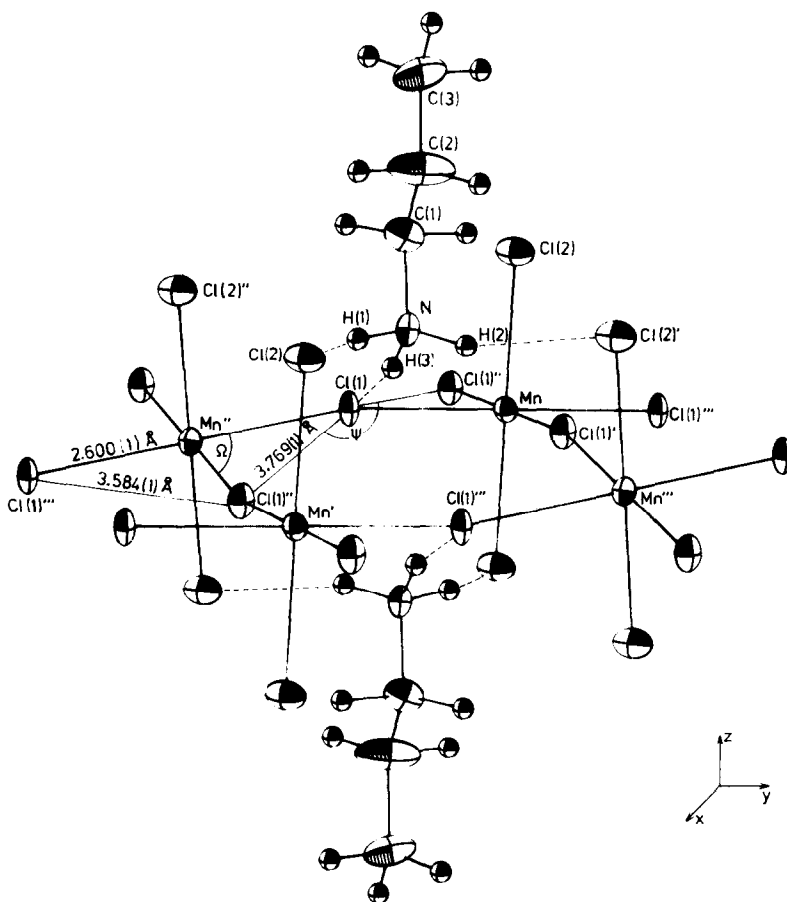
FIG. 1. Part of the structure of $\delta$-$(C_3H_7NH_3)_2MnCl_4$ showing the attachment of two propylammonium ions to the perovskite-like layer via hydrogen bonds. On each side of the layer only one mirror-related propylammonium group with the corresponding hydrogen bonds is shown.

Cd ($13$) the low-temperature to room-temperature phase transitions have been reported. In Ref. ($12$) it was shown that the hydrogen bonding scheme for compounds with $n > 1$ is different from that with $n = 1$ for steric reasons. Therefore, the transition behavior must also be different for compounds with $n = 1$ or $n > 1$. For the propyl compound, the Mn and Cd derivatives differ appreciably in their phase-transition behavior ($14, 15$). The structure of the $\delta$-phase of $(C_3H_7NH_3)_2MnCl_4$ has been reported ($16, 17$), and for the Cd compound the 183°K transition has been explained ($18$).

The room-temperature structure of $(C_{10}H_{21}NH_3)_2MnCl_4$ has also been reported ($19$). During the author's work in these laboratories with the various phases of $(C_3H_7NH_3)_2MnCl_4$, he learned that the propyl compound in the series $(C_nH_{2n+1}NH_3)_2MnCl_4$ has some unique properties. Some results for this compound are presented here, and a possible reason for its remarkable stability is given. Hereafter, the self-explanatory abbreviations C1Mn, C2Mn, C3Mn, etc., will be used. The term "hydrogen bond" will be abbreviated as "h.b."
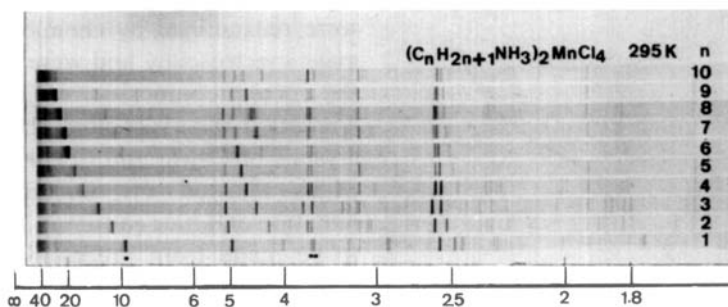
FIG. 2. Guinier photograph for $(C_nH_{2n+1}NH_3)_2MnCl_4$ with $n = 1$–10. The marked reflexions are 002, 200, and 020.

## Experimental

Crystals of C1Mn, C2Mn, and C3Mn were obtained by evaporation of water/ethanol solutions of $MnCl_2$ and the respective commercially available alkylammonium chlorides. The higher homologs were obtained by reacting the appropriate alkylamine, dissolved in i–$C_3H_7OH$, with hydrogen chloride, and subsequent precipitation with $MnCl_2$ solution followed by recrystallization from alcoholic solution. For the powder X-ray work the crystals or precipitates were carefully ground, and the powders were embedded in Cellit L 700. This matrix provided flat and smooth samples and prevented or, at least, delayed

thermal decomposition at high temperature. $CuK\alpha_1$ radiation from a Johansson monochromator was used throughout this work, with silicon as internal standard. The powder photograph of C1Mn–C10Mn (Fig. 2) shows the pattern of 10 samples taken at room temperature. The positions of the powder diffraction lines were measured with a traveling microscope, and unit-cell parameters were obtained by least-squares refinements (20). The results for C1Mn–C9Mn are given in Table I and Fig. 3. In Fig. 4, the normalized differences $(a - b)/b$ are shown. The space group $Abma$ and the lattice constants for $n = 1$–5 have been confirmed by single-crystal work. Some of the values found for the lattice constants

TABLE I

UNIT-CELL PARAMETERS, UNIT-CELL VOLUMES, VOLUME INCREASE FOR $(C_nH_{2n+1}NH_3)_2MnCl_4$ WITH $n = 1$–9 AT 295°K, AND TRANSITION TEMPERATURES TO THE ZERO-TILT PHASES (FROM GUINIER PHOTOGRAPHS)[a]

| $n$ | $a$ (Å) | $b$ (Å) | $c$ (Å) | $V$ (Å$^3$) | $\Delta V$ (Å$^3$) | $T_c$ (°K) |
|---|---|---|---|---|---|---|
| 1 | 7.263(2) | 7.202(2) | 19.388(8) | 1014.15 | | 398 |
| 2 | 7.352(2) | 7.258(3) | 22.085(9) | 1178.47 | 164.3 | 424 |
| 3 | 7.468(2) | 7.247(2) | 25.798(20) | 1396.20 | 217.7 | 451 |
| 4 | 7.342(5) | 7.257(5) | 31.87(12) | 1698.06 | 301.9 | 382 |
| 5 | 7.352(4) | 7.265(4) | 35.60(6) | 1901.48 | 203.4 | 382 |
| 6 | 7.34(1) | 7.25(1) | 39.80(15) | 2117.96 | 216.5 | 375 |
| 7 | 7.33(1) | 7.28(1) | 41.78(21) | 2229.48 | 111.5 | 375 |
| 8 | 7.345(6) | 7.270(6) | 45.08(8) | 2407.19 | 177.7 | 360 |
| 9 | 7.342(5) | 7.267(5) | 51.54(15) | 2749.88 | 342.7 | 356 |

[a] Space group $Abma$ is confirmed for $n = 1$–5 and assumed for $n = 6$–9.
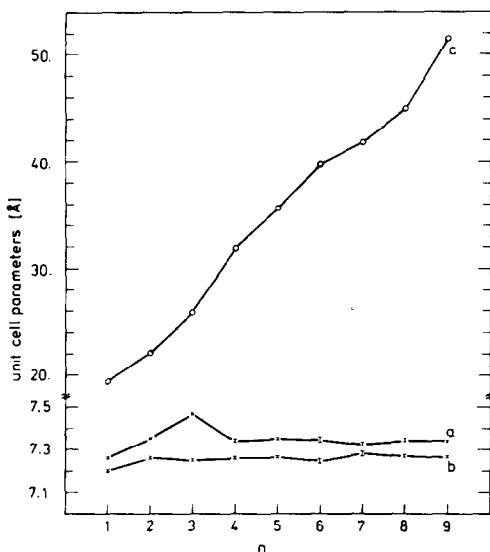
FIG. 3. Unit-cell parameters vs $n$.

were strikingly different compared with those given in $(21)$. Thus, the long axes were found to be 31.87 (28.61), 35.60 (31.95), and 39.80 (36.63) Å for $n = 4, 5, 6$ [values from $(21)$ in parentheses]. Consequently, the samples with $n = 4$ and 5 used for this work
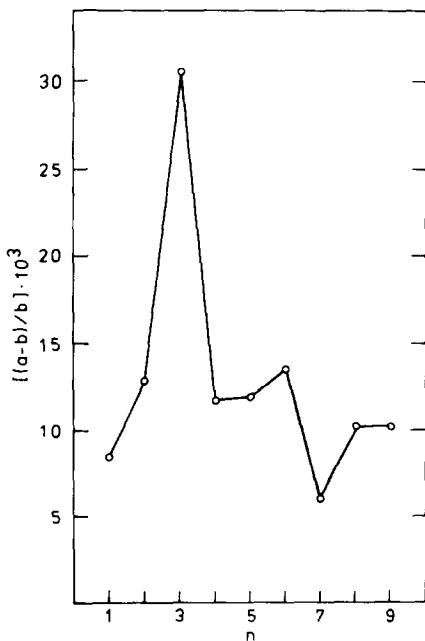


FIG. 4. Normalized differences $(a - b)/b$ [$\times 10^3$] vs $n$.

were reexamined by chemical analysis and mass spectroscopy and were shown to have the correct composition. During this reexamination relatively small, but good, single crystals of C4Mn and C5Mn were detected which allowed the unambiguous determination of lattice constants and space group to be made from precession photographs. (The structure determination has been completed for C4Mn). From the similarities of the powder patterns for $n = 4-9$ and the successful indexing of the patterns of C6Mn–C9Mn, the space group $Abma$ was also assumed to be correct for the higher members to $n = 9$.

To obtain the transition temperatures, the Guinier chamber was used with a temperature-controlled heating device. The temperature stability was better than 1°K. Since the temperature gradient within the U-shaped heating zone is very important, the sample holder was constructed from a Ni–CrNi thermocouple and the temperatures registered by the thermocouple were taken as those of the sample. From the known transition temperatures of C1Mn–C3Mn $(1)$, the difference between the real transition temperatures and the registered temperatures was taken to be 5°K and the reported values were corrected accordingly. The transition to the high-temperature zero-tilt phase was assumed to have taken place when the reflections 200 and 020 (cf. Fig. 2) were no longer distinguishable. The results for $n = 1-9$ are plotted in Fig. 5.

## Discussion

The compound C3Mn is unique among the members of the whole series with respect to several properties. In particular, the compound exhibits the greatest difference between the $a$ and $b$ lattice constants at room temperature (Figs. 2, 3, 4) and a value of the Mn–Cl(1) (in-plane chlorine) which appears to be the largest one ever found. It shows the highest temperature of transition to a
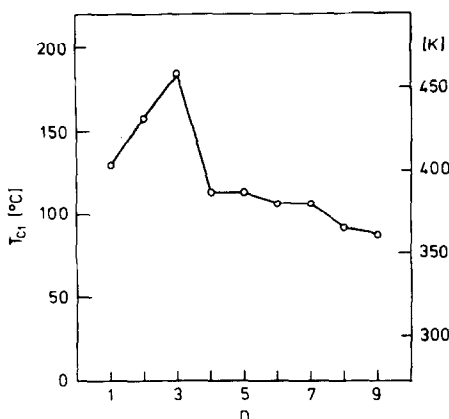
FIG. 5. Temperatures of transitions to the high-temperature zero-tilt phases as obtained from Guinier photographs.

zero-tilt phase, i.e., a phase for which the powder-diffraction lines corresponding to $a$ and $b$ (e.g., 200 and 020) have merged to give one single line (this does not necessarily mean that the corresponding phase is tetragonal, as it is in the case of C1Mn–C3Mn). Furthermore, the stability range of the disordered h.b. system (which is typical for the room-temperature phases) is much greater for C3Mn than for C2Mn. This range is 225 to 424°K for C2Mn, and at least 110 to 451°K for C3Mn.

These properties must be related with some structural features which distinguish C3Mn from the other members of the series. We note at once that the C10Mn and C1Mn compounds can both be excluded from the series for the following reasons. First, C10Mn is monoclinic $(P2_1/a)$. It is different from the other members in that, indeed, it is built similar to C3Mn, but the alkyl residue shows a paraffinic packing (19) which does not allow the space group $Abma$. We can assume that the members of the series with $n > 9$ behave like C10Mn and that their structures are determined by their paraffinic packing.

Figure 1 shows the connection of the $R$NH₃ residues to the perovskite-like layer via N–H···Cl h.b. The mirror plane of $Abma$

passes through Mn and Mn′ with atoms Cl(2) and N being almost in it. Considering the time average and the operation of the mirror plane, the $R$NH₃ group (Fig. 1) and its mirror image (which is not shown) are both present in the structure with equal probabilities. The same is true for the h.b. scheme shown in Fig. 1 and its mirror image. Both the $R$NH₃ group and the h.b. scheme are dynamically disordered (22). Now, the h.b. scheme of Fig. 1 does not apply to C1Mn (10–12). In contrast to C3Mn, in which one h.b. runs to a bridging chlorine atom and two h.b. run to axial chlorine atoms ["$aab$" h.b. scheme (23)], C1Mn has two h.b. running to bridging chlorine atoms and one running to an axial atom ($abb$ h.b. scheme). Thus, C1Mn is also not comparable to C3Mn. Since C10Mn has already been excluded, the series of comparable compounds is considered to extend from C2Mn to C9Mn. The space group of the room-temperature phases of C2Mn to C5Mn—$Abma$ (No. 64)—is assumed to be valid also for C6Mn to C9Mn.

Although the compounds C2Mn–C9Mn have essentially the same structure with disordered alkyl chains and h.b. schemes, there are some significant differences. These differences will now be summarized and used to provide a possible explanation for the observed physical properties.

A striking difference between the C2Mn and C3Mn compounds pertains to the location of the terminal methyl groups. For C3Mn this group lies almost in the mirror plane (17), whereas for C2Mn it is far removed from this plane [about 0.35 Å (23)]. The reason for this deviation is the $aab$-h.b. scheme, which forces the alkyl-ammonium groups into an oblique orientation with respect to the mirror plane. Together with the all-$trans$ conformation (for C2Mn and C3Mn), this orientation results in a zig-zag conformation of the alkyl chain with respect to the mirror plane (i.e., if one C atom lies on one side, then the next one lies on the other side). The different

distance from the mirror plane has consequences for the packing of the terminal methyl groups, i.e., packing of the neutral strata. This situation is shown in Fig. 6 for C2Mn and in Fig. 7 for C3Mn. In Fig. 6 we note that each pair of mirror-related methyl groups is surrounded by four other pairs at a different height (i.e., they belong to the neighboring stratum) and, in addition, by four pairs which belong to the same stratum. For a methyl group, the accepted value for the van der Waals radius is 2.0 Å. We may, therefore, assume that nearest neighbors have a separation of about 4 Å. Considering the central pair of methyl groups in Fig. 6, we assume that at a given time the methyl group is at position I, for which all distances of about 4 Å are shown. There are five nearest

neighbors with distances between 4.08 and 4.19 Å which are marked by I. When the central methyl group moves to position II, the groups marked by II are the five nearest neighbors. For C2Mn this mode of neighboring results in (i) different neighboring groups for positions I and II and (ii) a coupling of the movements about the $y$ direction which causes a coupling of the movements between neighboring strata. This movement must be cooperative. Moreover it is not merely van der Waals interaction which connects neighboring strata.

The situation for the room temperature phase of C3Mn is quite different (Fig. 7). In this case there is only little movement of the methyl groups across the mirror plane and the mirror-related position is reached by
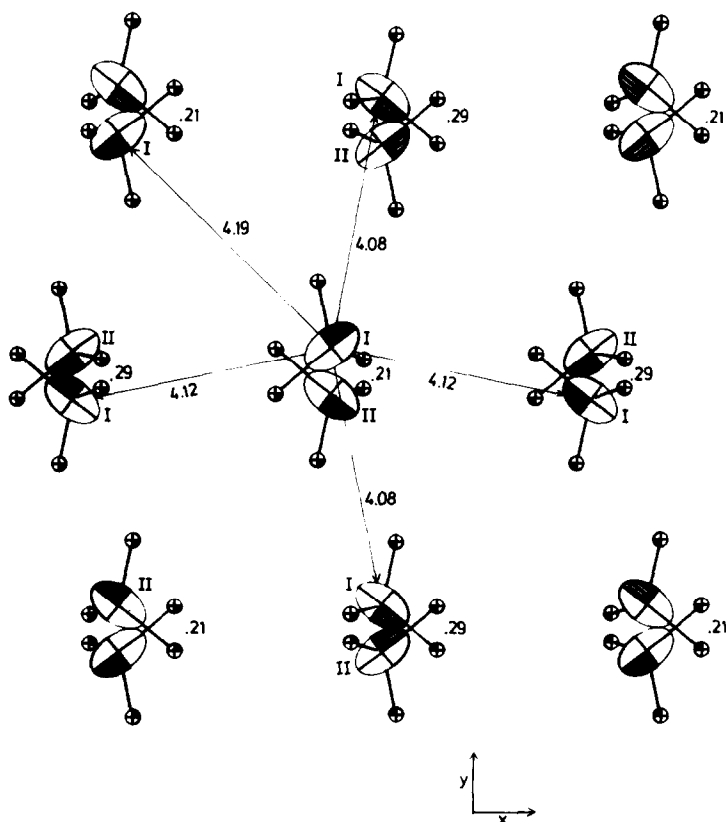


FIG. 6. Interstrata contact and packing mode for $\beta$-$(C_2H_5NH_3)_2MnCl_4$ at 295°K with contact distances for positions I and height in $z$.
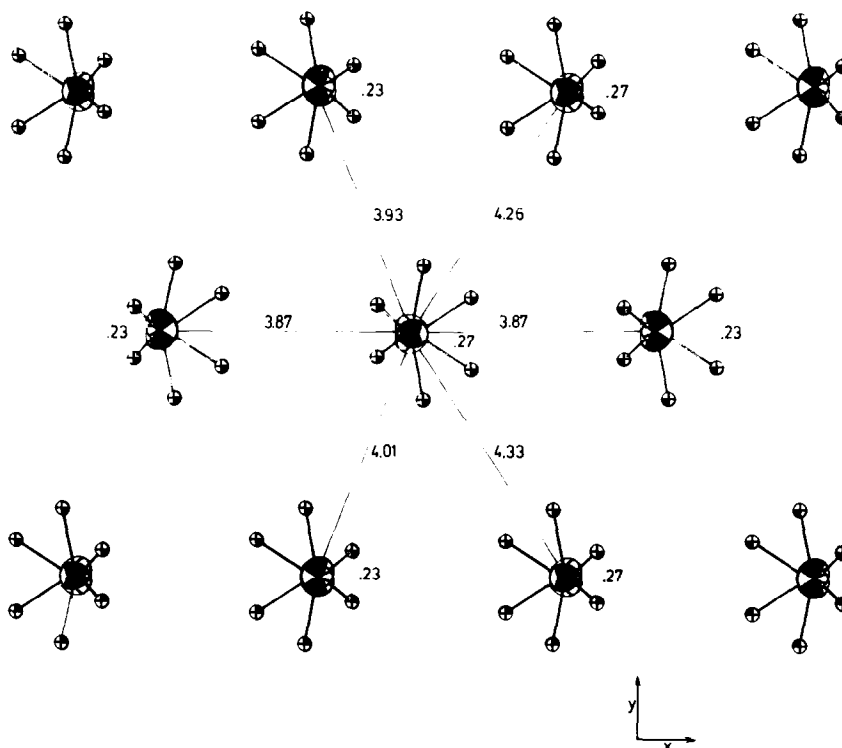
FIG. 7. Interstrata contact and packing mode for $\delta$-$(C_3H_7NH_3)_2MnCl_4$ at 180°K with contact distances (Å) and height in $z$.

rotation about the long molecule axis. This results in a quite different packing mode which has four nearest neighbors (at distances 3.87 to 4.01 Å) from the neighboring stratum and two nearest neighbors from the same stratum with longer distances (4.26 and 4.33 Å). For C3Mn, the transition from one stratum to another is much smoother since there is less coupling between the motions of the different strata.

Compound C4Mn is different from both C2Mn and C3Mn. It no longer has the all-*trans* conformation for the alkyl chain, but a *trans-gauche* conformation in which the terminal methyl group is rotated out of the plane of the other C atoms. This again leads to a neighboring which is less favorable than it is for C3Mn. The very similar powder patterns of C4Mn–C9Mn (Fig. 2) and the almost uniform transition temperatures (Fig.

5) for these compounds make it reasonable to take C4Mn as a representative of these six compounds.

With diffraction methods it is not possible to distinguish between dynamical and static disorder. However, it is known from the nuclear resonance analysis of the corresponding Cd compounds (22) that the disorder of the alkyl chains is of the dynamical kind. Consequently, the mirror plane of space group *Abma* requires the alkylammonium group to move across the mirror plane in order to reach the mirror-related position. This kind of movement is different for C2Mn, C3Mn, and C4Mn. It is simplest for the room-temperature phase of C3Mn, where it corresponds to a rotation about the long molecule axis through N and the terminal atom C(3). The ethylammonium group of C2Mn may also be represented by

the long molecule axis through N and C(2). Unlike C3Mn, the movement into the symmetry-related position requires not only a rotation, but, in addition, a flipping motion of the molecule axis as a whole. It has already been noted that this flipping must be cooperative. The movement of C4Mn is even more complicated; this molecule, with N–C(3) all-*trans* and C(4) *gauche*, must undergo a rotation about the long molecule axis through N and the last but one C atom C(3) and a flipping of this axis as in the case of C2Mn. In addition, it is necessary to rotate about the C(2)–C(3) bond in order to put C(4) into the right mirror-related position.

With this interpretation of the diffraction results, one can argue that C3Mn has one degree of freedom of motion, C2Mn has two, and C4Mn three of them. This point of view may be applied to the results of the measurements of the transition temperatures (Fig. 5). These values may be interpreted as follows: Compound C3Mn, with only one degree of freedom, needs the largest amount of heat to reach its final state (with "molten" alkyl chains), and C4Mn needs less heat than does C2Mn to reach this state. The slight decrease of the temperature of transition with increasing $n$ could be correlated with the increase of internal motion produced in higher alkyl chains at room temperature. The latter argument, however, holds only as long as the assumed type of disorder is present. If the alkyl chains are ordered to produce the paraffinic packing as is the case for C10Mn, the transition temperature should increase with $n$ due to increasing van der Waals interaction. In fact, this behavior has been found for the long-chain molecules (25, 26).

The influence of the h.b. scheme on the tilt system of the perovskite-like layer, which has been discussed in detail elsewhere (27, 12), is only briefly considered here. On a time-average basis, each bridging Cl(1) atom takes part in two h.b., whereas each axial Cl(2) atom takes part in four h.b. of two

different types. By the operation of the N–H(1)···Cl(2) h.b. and its mirror image, Cl(2) is attracted toward N, thereby forcing the atoms Cl(1)″ and Cl(1)‴ to be below the level of the Mn atoms (at $z = 0.5$). A reverse operation raises Cl(1) and Cl(1)′ above the Mn level. This operation is supported by the N–H(3)···Cl(1) and $N_m$–H(3)$_m$···Cl(1)′ h.b. (index m means mirror related). The h.b. N–H(2)···Cl(2)′ and $N_m$–H(2)$_m$···Cl(2)″ cancel each other so that they do not influence the tilt system. At higher temperatures all members undergo structural phase transitions (provided that no thermal decomposition has taken place) and, finally, form phases in which no resulting tilt system is retained. Nuclear resonance analysis of the Cd compounds (22) has shown that the high-temperature phases are superpositions of up to eight h.b. schemes. It is highly probable that this is also the case for the manganese compounds. These h.b. are fully disordered and their influence on the octahedra layer is canceling, so that no resulting tilt system is observable. The corresponding phases may be called zero-tilt phases. In the zero-tilt phases, the $a$ and $b$ lattice constants are of equal length and probably identical (if the symmetry is tetragonal). This is not true for the room-temperature phases. By virtue of the influence of the h.b., the $MnCl_6$ octahedra are not only tilted but are also slightly distorted. The square base of an undistorted octahedron (or, more correctly, a tetragonal bipyramid since bonds to bridging and axial chlorine atoms are not of equal length) becomes a rectangle (cf. Fig. 1). The influence of this type of h.b. is such that $a$ is lengthened and $b$ is shortened; $a$ and $b$ depend on three variables (space group *Abma* still assumed): (i) the Mn–Cl(1) bond length $L$; (ii) the angle $\Omega$, e.g., $\angle$Cl(1)–Mn″–Cl(1)″, which describes the distortion of the square base; and (iii) the angle $\Psi$, e.g., $\angle$Cl(1)″–Cl(1)–Cl(1)″, which describes the washboard-like puckering of the octahedra layer.
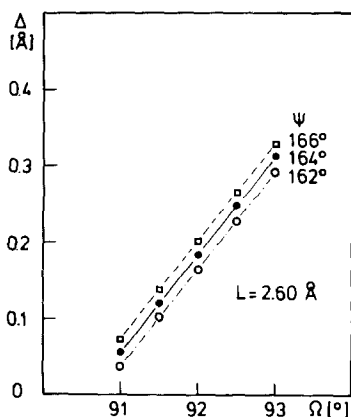
FIG. 8. $\Delta$ vs $\Omega$ for three values of $\Psi$, with fixed value of $L$.

Regarding the tilt system of the room-temperature phases $[a^-a^-c^0 (6, 1)]$, the difference between $a$ and $b$ is given by the following expression on the basis of simple geometric considerations.

$$\Delta = a - b = 2L\{[(1-\cos\,\Psi)(1-\cos\,\Omega)]^{1/2}$$
$$-[2(1+\cos\,\Omega)]^{1/2}\}.$$

The dependence of $\Delta$ on $L$, $\Psi$, and $\Omega$ is such that $\Omega$ has the greatest influence on $\Delta$. To a good approximation, the greater the deviation of $\Omega$ from 90°, the larger is $\Delta$ (cf. Fig. 8). Table II lists values of $\Delta$, $L$, $\Psi$, and $\Omega$ for some known structures to demonstrate these relationships. Obviously, C3Mn has the greatest octahedron distortion angle $\Omega$

and, consequently, the largest $\Delta$. From Fig. 3 and Table II it is clear that the outstanding difference $\Delta$ for C3Mn depends on its large value of $\Omega$. However, since $b$ depends only on $\Omega$ and $L$ and changes inversely to $a$ (which is even, in addition, reduced by $\Psi$), one would expect $b$ for C3Mn to have by far the smallest value in the whole series. Since this is not true, one must assume that C3Mn has the greatest bond length $L$. In fact, it is known from single crystal work that the Mn–Cl(1) bond length for C3Mn (16) appears to be the largest one reported to date (28).

If a chlorine atom is the acceptor for a h.b., this interaction may be considered a coordination contact, from which it follows that the neighboring Mn–Cl bond is somewhat weakened and, consequently, lengthened. The amount of lengthening should depend on the h.b. strength. It is immediately apparent that an increased h.b. strength will increase the variables $L$, $\Omega$, and $\Psi$ which define $\Delta$. If we take the normalized difference as $(a-b)/b$, its value is independent of the bond length $L$. If we accept this value (cf. Fig. 4) as a qualitative measure for the h.b. strength of the compound under consideration, it is clear that C3Mn possesses the greatest h.b. strength. It is also to be noted that the h.b. strength decreases with increasing temperature. One would, therefore, expect that the values of $(a-b)/b$ also decrease with increasing temperature.

TABLE II

$\Delta$, $L$, $\Psi$, AND $\Omega$ FOR SOME KNOWN STRUCTURES FROM REFINEMENTS OF DIFFRACTOMETER DATA

| Compound (reference) | Radiation | $T$ (°K) | $\Delta$ (Å) | $L$ (Å) | $\Psi$ (°) | $\Omega$ (°) |
|---|---|---|---|---|---|---|
| $\delta$-$(C_3H_7NH_3)_2MnCl_4$ (17) | N | 180 | 0.289 | 2.600(0) | 163.3 | 92.9 |
| $\delta$-$(C_3H_7NH_3)_2MnCl_4$ (16) | X | 295 | 0.220 | 2.629(5) | 164.4 | 92.3 |
| $\beta$-$(C_2H_5NH_3)_2MnCl_4$ (29) | N | 293 | 0.095 | 2.593(0) | 166.03 | 91.2 |
| $\gamma$-$(C_2H_5NH_3)_2MnCl_4$ (12) | X | 126 | 0.174[a] | 2.579[b] | 162.49 | 91.88 |
| $(C_4H_9NH_3)_2MnCl_4$ (24) | X | 294 | 0.084 | 2.588(1) | 166.52 | 91.06 |

[a] $b$ reduced by an additional $c$ tilt.
[b] Mean value.

Figure 9 shows this temperature dependence for C3Mn. It is clearly seen that the value for this compound decreases from a very large magnitude at low temperatures to the room-temperature value, which is unique in comparison with those of the other members. Only at 400°K is $(a - b)/b$ for C3Mn of the same magnitude as are the room-temperature values for the other members. At this temperature, however, all other members of the series except C2Mn have already undergone their phase transition to the zero-tilt phase.

Different h.b. strength is detectable by the measurement of the appropriate bond lengths in the N–H··Cl region. At present only the room-temperature phases of C2Mn, C3Mn, and C4Mn are known, with C3Mn and C4Mn having been investigated by X-ray methods, and the C2Mn compound by neutron diffraction as well. Owing to the high thermal disorder and the incoherent scattering of hydrogen in the neutron measurement, the calculated distances and angles are rather inexact and do not allow final conclusions concerning the bond strengths. Careful ir studies of the N–H stretching frequencies
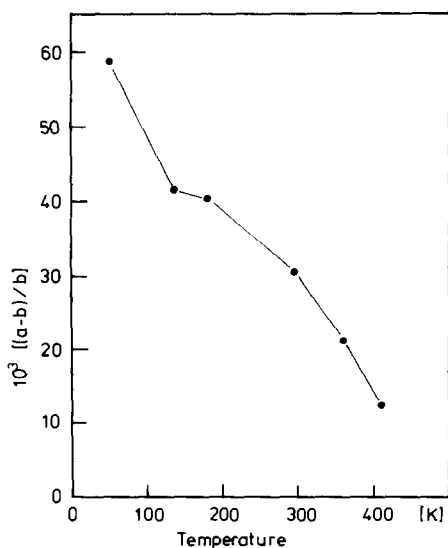
may be able to provide information about this question.

If the conclusion is accepted that the difference in $\Delta$ for C2Mn–C9Mn is due to different h.b. strengths, and it is noted that the type of h.b. is the same at least for C2Mn–C4Mn, the different strengths can be described qualitatively in terms of higher and lower temperatures. Thus, the weaker a h.b. is, the higher is its virtual ambient temperature and the nearer is the transition point to the zero-tilt phase.

To show this relation for C2Mn–C4Mn, room-temperature, single-crystal diffractometer data were refined in the same manner: all atoms anisotropic, Cl(2), N, and C on the mirror plane (except C(4) of C4Mn), with no hydrogen atoms involved. The root mean-square displacements for N, Cl(1), and Cl(2) are shown in Table III. These values are inversely proportional to the transition temperatures, as well as to the normalized differences of Fig. 4. The conclusion seems to be justified that the increased movement of the alkyl chains of C2Mn and C4Mn results in a "higher ambient temperature" for the corresponding h.b. than is the case for C3Mn. Therefore, these compounds have the lower transition temperatures and smaller values of $\Delta$.

Finally, it should be noted that the favorable packing of C3Mn at room temperature



FIG. 9. Temperature dependence of $(a - b)/b[\times 10^3]$ for $(C_3H_7NH_3)_2MnCl_4$.

TABLE III

ROOT-MEAN-SQUARE DISPLACEMENTS (Å) FOR ATOMS Cl(1), AND Cl(2) AND N FOR C2Mn, C3Mn, AND C4Mn AT ROOM TEMPERATURE

|       | RMSD | C2Mn  | C3Mn  | C4Mn  |
|-------|------|-------|-------|-------|
| Cl(1) | 1    | 0.149 | 0.158 | 0.159 |
|       | 2    | 0.180 | 0.177 | 0.214 |
|       | 3    | 0.259 | 0.194 | 0.321 |
| Cl(2) | 1    | 0.168 | 0.134 | 0.225 |
|       | 2    | 0.227 | 0.155 | 0.266 |
|       | 3    | 0.295 | 0.249 | 0.298 |
| N     | 1    | 0.168 | 0.119 | 0.210 |
|       | 2    | 0.243 | 0.209 | 0.239 |
|       | 3    | 0.247 | 0.239 | 0.271 |

$(C_3H_7NH_3)_2MnCl_4$

endothermic   $\frac{dq}{dt}$   exothermic

$\left[ 0.5\ \frac{mcal}{s} \right.$   20 K/min

| $\zeta$ Pbca | $\varepsilon$ Pbma | $\delta$ Abma | $\delta$ Abma | $\gamma$ Abma substructure | $\beta$ Abma | $\alpha$ I4/mmm |
|---|---|---|---|---|---|---|
| a = 7.457 Å | a = 7.443 Å | a = 7.458 Å | a = 7.468 Å | a = 7.442 Å | a = 7.421 Å | a = $\sqrt{2}\times7.4$ Å |
| b = 7.043 | b = 3×7.142 | b = 7.169 | b = 7.247 | b = 7.289 | b = 7.337 | b = $\sqrt{2}\times7.4$ |
| c = 25.255 | c = 25.422 | c = 25.610 | c = 25.798 | c = 26.460 | c = 27.357 | c = 27.5 |
| at 48 K | at 136.5 K | at 182 K | at 295 K | at 358 K | at 410 K | |

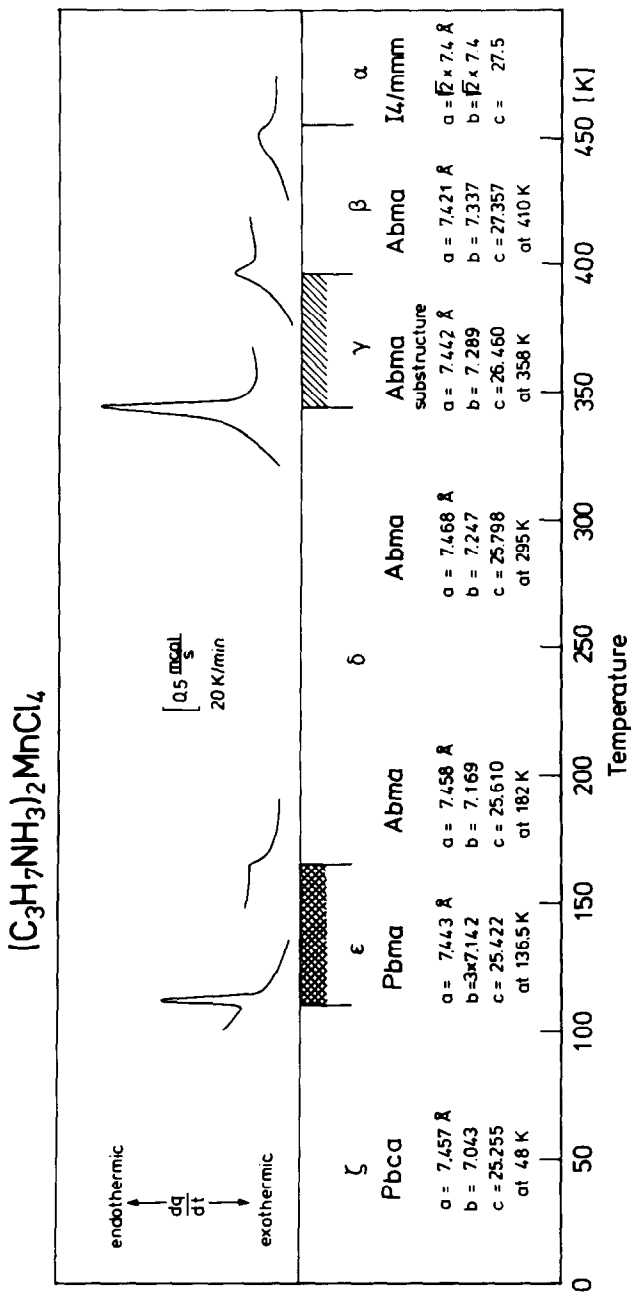Temperature: 0   50   100   150   200   250   300   350   400   450 [K]

FIG. 10. Phases of $(C_3H_7NH_3)_2MnCl_4$ with space groups, lattice constants, and DTA characteristics for the transitions. Ranges of commensurate and incommensurate superstructures are indicated by cross-hatched and hatched areas, respectively.

is evidently not retained up to the transition temperature. This is shown by an investigation of its $\gamma$- and $\beta$-phase, which is in progress. It is probable that the formation of commensurate and incommensurate superstructures in C3Mn can be explained only by taking the interactions of the terminal methyl groups into account. A schematic view of the different phases of C3Mn with some of their characteristics is presented in Fig. 10.

## Acknowledgments

## References

1. W. DEPMEIER, J. FELSCHE, AND G. WILDER-MUTH, *J. Solid State Chem.* **21**, 57 (1977).
2. L. H. DE JONGH AND A. R. MIEDEMA, *Advan. Phys.* **23**, 1 (1974).
3. F. H. M. MISCHGOFSKY, Ph.D. Thesis, "Technische Hogeschool Delft (1977).
4. G. HEGER, "Habilitationsschrift," Marburg/Lahn (1978).
5. A. LEHNINGER, "Biochemistry," Worth, New York (1970).
6. A. M. GLAZER, *Acta Crystallogr.* B **28**, 3384 (1972).
7. G. CHAPUIS, H. AREND, AND R. KIND *Phys. Status Solidi A* **31**, 449 (1975).
8. G. CHAPUIS, R. KIND, AND H. AREND, *Phys. Status Solidi A* **36**, 285 (1976).
9. J. SELIGER, R. BLINC, R. KIND, AND H. AREND, *Z. Phys. B* **25**, 189 (1976).
10. G. HEGER, D. MULLEN, AND K. KNORR, *Phys. Status Solidi A* **31**, 455 (1975).
11. G. HEGER, D. MULLEN, AND K. KNORR, *Phys. Status Solidi A* **35**, 627 (1976).
12. W. DEPMEIER, *Acta Crystallogr.* B **33**, 3713 (1977).
13. G. CHAPUIS, *Phys. Status Solidi A* **43**, 203 (1977).
14. W. DEPMEIER, presented at the Informal Meeting on Halide Perovskite Layer Structures, Zürich (1976).
15. G. CHAPUIS, presented at the Informal Meeting on Halide Perovskite Layer Structures, Zürich (1976).
16. E. R. PETERSON AND R. D. WILLET, *J. Chem. Phys.* **56**, 1879 (1972).
17. W. DEPMEIER AND S. A. MASON, *Acta Crystallogr. B* **34**, 920 (1978).
18. G. CHAPUIS, *Acta Crystallogr. B* **34**, 1506 (1978).
19. M. R. CIAJOLO, P. CORRADINI, AND V. PAVONE, *Gazz. Chim. Ital.* **106**, 807 (1976).
20. D. SCHWARZENBACH, "Latcon. A General Program for the LS-Refinement of Lattice Constants," ETH, Zürich (1971).
21. A. DAOUD, A. THRIERR-SOREL, R. PERRET, AND B. CHAILLOT, *Rev. Roumaine Chim.* **22**, 857 (1977).
22. R. BLINC, M. BURGAR, B. LOŽAR, J. SELIGER, I. SLAK, V. RUTAR, H. AREND, AND R. KIND, *J. Chem. Phys.* **66**, 278 (1977).
23. W. DEPMEIER AND G. HEGER, *Acta Crystallogr. B* **34**, 1698 (1978).
24. W. DEPMEIER AND G. CHAPUIS, *Acta Crystallogr.* **B35**, in press.
25. M. VACATELLO AND P. CORRADINI, *Gazz. Chim. Ital.* **103**, 1027 (1973).
26. M. VACATELLO AND P. CORRADINI, *Gazz. Chim. Ital.* **104**, 773 (1974).
27. R. D. WILLET AND E. F. RIEDEL, *Chem. Phys.* **8**, 112 (1975).
28. "Bidics—Bond Index to the Determination of Inorganic Crystal Structures," Institute for Materials Research, McMaster University, Hamilton, Ontario, Canada (1970–1976).
29. W. DEPMEIER, *Acta Crystallogr. B* **32**, 303 (1976).